Establishment of different plasmid only-based reverse genetics systems for the recovery of African horse sickness virus

Andelé M. Conradie[a], Liesel Stassen[a], Henk Huismans[b], Christiaan A. Potgieter[c,d] and Jacques Theron[a]*

[a] Department of Microbiology and Plant Pathology, University of Pretoria, Pretoria 0002, South Africa

[b] Department of Genetics, University of Pretoria, Pretoria 0002, South Africa

[c] Deltamune (Pty) Ltd, Lyttelton, Centurion, South Africa

[d] Department of Biochemistry, Centre for Human Metabonomics, North-West University, Potchefstroom, South Africa

***Corresponding author:** Prof Jacques Theron
Email: jacques.theron@up.ac.za
Telephone: +27 12 420-2994
Fax: +27 12 420-3266

ABSTRACT

In an effort to simplify and expand the utility of African horse sickness virus (AHSV) reverse genetics, different plasmid-based reverse genetics systems were developed. Plasmids containing cDNAs corresponding to each of the full-length double-stranded RNA genome segments of AHSV-4 under control of a T7 RNA polymerase promoter were co-transfected in cells expressing T7 RNA polymerase, and infectious AHSV-4 was recovered. This reverse genetics system was improved by reducing the required plasmids from 10 to five and resulted in enhanced virus recovery. Subsequently, a T7 RNA polymerase expression cassette was incorporated into one of the AHSV-4 rescue plasmids. This modified 5-plasmid set enabled virus recovery in BSR or L929 cells, thus offering the possibility to generate AHSV-4 in any cell line. Moreover, mutant and cross-serotype reassortant viruses were recovered. These plasmid DNA-based reverse genetics systems thus offer new possibilities for investigating AHSV biology and development of designer AHSV vaccine strains.

Keywords:

African horse sickness virus; orbivirus; reverse genetics; dsRNA; *Reoviridae*; virus rescue; T7 RNA polymerase; reassortment

Introduction

African horse sickness (AHS), of which African horse sickness virus (AHSV) is the causative agent, is one of the most lethal systemic diseases of horses with a mortality rate in naïve animals up to 95% (Stassen et al., 2014). The virus is transmitted primarily by certain species of biting midges in the genus *Culicoides*, which become infected after taking a blood meal from an infected viraemic host (Mellor et al., 2000; Venter et al., 2009). Although AHS is endemic in sub-Saharan Africa, outbreaks with devastating effects have occurred in North Africa, the Middle East, the Arabian Peninsula and southern Europe (Howell, 1960; Rafyi, 1961; Diaz Montilla and Panos Marti, 1967; Lubroth, 1988; Rodriquez et al., 1992; Portas et al., 1999). Different factors such as climate change (Purse et al., 2008; Tabachnik et al., 2010) and increased international trade and movement of animals (MacLachlan and Guthrie, 2010; Martinez-Lopez et al., 2011) have raised concerns that AHSV may be re-introduced in European countries. Due to the economic impact of disease outbreaks, severity of disease in

horses, and its capacity for sudden and rapid expansion, AHS is listed by the World Organization for Animal Health (OIE) as a notifiable equine disease.

AHSV is a member of the genus *Orbivirus* within the family *Reoviridae*. Like other members of this genus, AHSV is non-enveloped and has a complex capsid structure (Manole et al., 2012). The virion is comprised of two concentric protein shells surrounding the genome of 10 linear segments of double-stranded (ds) RNA, which are designated from segment 1 (S1) to S10 in decreasing order of size (Bremer et al., 1990). The outer capsid comprises two proteins, VP2 and VP5, which together form a continuous layer that covers the inner capsid or core. The core particle is composed of two major (VP3 and VP7) and three minor (VP1, VP4 and VP6) proteins, in addition to the dsRNA genome (Manole et al., 2012). The outer capsid proteins are removed during cell entry and transcriptionally active core particles are released into the cytosol where virus replication occurs (Forzan et al., 2007). Within the core particle, each of the dsRNA genome segments are repeatedly transcribed by the core-associated enzymes VP1 (RNA-dependant RNA polymerase), VP4 (capping-enzyme) and VP6 (helicase), resulting in extrusion of newly synthesized capped viral single-stranded RNA (ssRNA). The extruded positive-sense transcripts have the dual function of serving as templates for the synthesis of viral proteins and for negative-sense RNA synthesis during dsRNA replication (Mertens and Diprose, 2004; Patel and Roy, 2014). In addition to the structural proteins, other AHSV-encoded proteins (NS1, NS2, NS3 and NS4) are also produced in infected cells where they are thought to be involved in virus replication, morphogenesis and release of progeny virus particles (Uitenweerde et al., 1995; van Staden et al., 1995; Maree and Huismans, 1997; Zwart et al., 2015). Although the veterinary (Guthrie, 2007; Clift and Penrith, 2010) and vaccine-related aspects of AHSV have received some attention (Scanlen et al., 2002; Guthrie et al., 2009; Alberca et al., 2014), AHSV replication and the role of individual viral proteins in this process, as well as AHSV-host cell interactions remain largely uncharacterized.

A reverse genetics system to engineer viable virus containing targeted sequence modifications has become an essential tool for the molecular dissection of viral gene products, studies regarding viral replication and pathogenesis, and for the development of vaccines. The development of a reverse genetics system for the *Reoviridae* family has lagged behind that of other RNA virus families due to technical complexities associated with the manipulation of multi-segmented dsRNA genomes (Komoto and Taniguchi, 2013; Trask et

al., 2013). Nevertheless, in recent years, reverse genetics systems have been developed for rotavirus (genus *Rotavirus*), reoviruses (genus *Orthoreovirus*), as well as AHSV, bluetongue virus (BTV) and epizootic haemorrhagic disease virus (EHDV) (genus *Orbivirus*) (Komoto et al., 2006; Kobayashi et al., 2007; Boyce et al., 2008; Kaname et al., 2013; Vermaak et al., 2015; Yang et al., 2015). For rotavirus, single gene replacement systems that require helper virus, selection, or both have been developed (Komoto et al., 2006; Trask et al., 2010; Troupin et al., 2010). In contrast, helper virus-independent reverse genetics systems have been established for reoviruses and orbiviruses. AHSV, BTV and EHDV can be recovered by the transfection of *in vitro*-transcribed and capped RNAs into permissive cell lines (Boyce et al., 2008; Vermaak et al., 2015) or into cells that had previously been transfected with helper expression plasmids that synthesize the core proteins and the two non-structural proteins NS1 and NS2 (Kaname et al., 2013; Matsuo and Roy, 2013; Yang et al., 2015). An entirely plasmid only-based reverse genetics system has been developed for mammalian orthoreovirus (Kobayashi et al., 2007) and, more recently, for BTV (Pretorius et al., 2015) and a fusogenic bat-borne orthoreovirus (Kawagishi et al., 2016). The development of reverse genetics has revolutionized the study of reoviruses (Dermody et al., 2013) and BTV (Roy, 2013) by providing a powerful tool for investigating virus replication and disease.

Here, we report the development of a plasmid-only reverse genetics system for AHSV-4 that allows for recovery of the virus from 10 cDNA clones representing the viral genome. We subsequently improved the basic AHSV-4 reverse genetics system by consolidating the viral genome segment cDNAs into five plasmids, which permits more efficient virus recovery compared to the 10-plasmid system. Finally, we increased the flexibility of the 5-plasmid reverse genetics system by including a T7 RNA polymerase expression cassette onto the genetic backbone of the reverse genetics plasmid, thus liberating the rescue of viable virus from its dependence on T7 RNA polymerase-expressing cell lines. The performance of the reverse genetics systems were validated by recovery of mutant and directed cross-serotype reassortant viruses. The enhancements reported here represent a significant advance for the application of reverse genetics to the study of AHSV.

Results

Construction of reverse genetics plasmids

Previous work from our laboratory established a reverse genetics system for the prototype orbivirus, BTV, using a bacteriophage T7 RNA polymerase system, whereby infectious virus could be generated reproducibly entirely from cDNA clones (Pretorius et al., 2015). In this study, we generated two reverse genetics plasmids, pJAD1 and pJAD2, as described under Materials and Methods. Both the pJAD1 and pJAD2 plasmids contain an identical transcription cassette, which was obtained from the pRG15 reverse genetics plasmid, and is flanked by newly introduced T7Te transcription terminators to prevent transcription into or out of the cloned DNA. Moreover, with a view to reducing the number of plasmids required for AHSV-4 recovery, unique restriction enzyme sites were also incorporated into the reverse genetics plasmids. In the case of pJAD1, unique *Stu*I restriction sites flanking the transcription cassette was incorporated, as well as a unique *Pme*I restriction site adjacent to the downstream T7Te terminator. In the case of pJAD2, unique *Pme*I restriction sites that flank the T7Te terminator sequences were incorporated (Fig. 1).

Plasmid-based reverse genetics of AHSV-4

To generate AHSV-4 from cloned cDNA, plasmids encoding each viral genome segment were engineered by incorporating cDNA copies of genome segments S1 through S5 into pJAD1 and cDNA copies of genome segments S6 through S10 into pJAD2. Each plasmid thus contains one full-length genome segment cDNA placed under control of the bacteriophage T7 RNA polymerase promoter and appended with the hepatitis delta virus (HDV) ribozyme at the 3' terminus. After transcription with T7 RNA polymerase, these plasmids are anticipated to generate 10 full-length positive-sense RNAs, each containing native 5'- and 3'-ends (Fig. 2A).

The 10 AHSV-4 constructs were co-transfected into BSR-T7 cells, which constitutively express T7 RNA polymerase. The cells were harvested 5 days post-transfection, lysed and plaque assays were performed on BSR cells. Plaques were recovered from cells transfected with the 10 AHSV-4 cDNA plasmids, indicating the presence of replicating virus. In contrast, no plaques were observed in control, mock-transfected cells (Fig. 2B). To confirm

virus recovery, individual plaques were picked, amplified in BSR cells and genomic dsRNA purified from infected cells was subsequently analyzed on a non-denaturing polyacrylamide gel. The electropherotype of plasmid-derived AHSV-4 was indistinguishable from that of wild-type AHSV-4 derived from cell infection (Fig. 2C).

To exclude the possibility that recovered AHSV-4 represents contamination by wild-type AHSV-4, a silent mutation (A to G at nucleotide 1010) resulting in the introduction of a unique *Pst*I site was introduced into the S5 genome segment by site-directed mutagenesis of the pJAD-S5 rescue plasmid. Since this change has not been observed in any reported AHSV S5 genome sequences, it thus serves as a signature for virus derived from plasmid-based rescue. The full-length S5 genome segment (1.748 kb) was amplified using RT-PCR of viral dsRNA extracted from BSR cells infected with either plasmid-derived AHSV-4 or wild-type AHSV-4. The S5 genome segment RT-PCR product derived from wild-type AHSV-4 was not digested with *Pst*I, whereas the S5 product from plasmid-derived AHSV-4 produced the expected DNA fragments of 1012 and 736 bp upon digestion. The nucleotide sequence of the purified amplicons were also determined, the results of which confirmed the presence of the unique *Pst*I restriction enzyme site in the S5 genome segment from plasmid-derived AHSV-4 (Fig. 2D).

To determine whether the plasmid-derived AHSV-4 and wild-type AHSV-4 have similar replication kinetics, BSR cells were infected with the respective viruses at a MOI of 0.1 pfu/cell and virus titres were determined at different times post-infection. There was essentially no difference in growth kinetics, and the titres of the plasmid-derived AHSV-4 and wild-type AHSV-4 were virtually identical at all the time points tested (Fig. 2E).

Taken together, the data indicate that AHSV-4 can be recovered entirely from plasmid cDNA and that the plasmid-derived virus retained the properties of wild-type AHSV-4.

Generation of a simplified reverse genetics system using five plasmids

Previous reports have indicated that a reduction in the number of plasmids required to rescue infectious virus may improve the efficiency of plasmid-based reverse genetics systems (Neumann et al., 2005; Zhang et al., 2009; Kobayashi et al., 2010). Thus, to reduce the number of plasmids required to rescue AHSV-4 by plasmid-based rescue, the AHSV-4 S6

through S10 genome segment transcription cassettes flanked by T7Te transcriptional terminators were recovered from the respective recombinant pJAD2 plasmids by digestion with *Pme*I and blunt-end cloned into the unique *Pme*I site of the recombinant pJAD1 plasmids (Fig. 1). The derived reverse genetics plasmids were designated pJAD-S1-S8, pJAD-S2-S6, pJAD-S3-S7, pJAD-S4-S10 and pJAD-S5-S9 (Fig. 3A). As expected, infectious AHSV-4 was recovered following plaque assays on BSR cell monolayers of the transfection cell lysate and subsequent characterization of the plaque-purified virus confirmed their plasmid origin (Figs. 3B-D).

Reassortant viruses based on the targeted exchange of specific genes may facilitate not only the functional mapping of genes, such as virulence factors, but also allow for the generation of vaccine strains of particular serotypes. Consequently, we attempted to modify AHSV-4 by exchange of the S2 and S6 genome segments of AHSV-4 with those of AHSV-1. The S2 and S6 genome segments encode for the outer capsid proteins VP2 and VP5, respectively. To this end, a dual reverse genetics plasmid was constructed, designated pJAD(A1)-S2-S6, which contained transcription cassettes of the S2 and S6 genome segments from AHSV-1. BSR-T7 cells were co-transfected with 5 plasmids in which the wild-type pJAD-S2-S6 construct was substituted with the pJAD(A1)-S2-S6 construct. Reassortant viruses from randomly selected plaques were amplified in BSR cells, dsRNA extracted and the genotype of the recovered viruses was determined by electrophoresis of the dsRNA on a non-denaturing polyacrylamide gel. The electrophoresis pattern of a representative reassortant virus, $_{A4}$AHSV-1$^{VP2/VP5}$, clearly shows co-migration of the S2 genome segment dsRNA with that of AHSV-1, but it was not possible to distinguish the origin of the S6 genome segment (Fig. 4A). However, since genome segment S6 of AHSV-4, but not the S6 genome segment of AHSV-1, has a distinctive *Bam*HI restriction site, the S6 genome segments of AHSV-4, AHSV-1 and the reassortant virus $_{A4}$AHSV-1$^{VP2/VP5}$ were amplified by RT-PCR and digested with *Bam*HI. When analyzed on an agarose gel, it was confirmed that the S6 genome segment of AHSV-4 was cleaved but not the S6 genome segments of AHSV-1 and the reassortant virus (Fig. 4B). The identity of the S2 and S6 genome segments of the reassortant virus as originating from AHSV-1 was furthermore confirmed by nucleotide sequencing of cDNA copies of the respective genome segments (data not shown). These results thus demonstrate the ability of the reverse genetics system to potentially generate reassortant viruses with any desired genetic combination between different AHSV strains or serotypes.

Generation of a modified 5-plasmid reverse genetics system that encodes both the AHSV-4 genome and T7 RNA polymerase

In both of the above reverse genetics systems, recovery of infectious AHSV-4 from plasmid DNA relies on the expression of T7 RNA polymerase within cells transfected with the AHSV-4 cDNA plasmids. Despite the success of both these approaches, they exclude the use of cells other than BSR-T7 cells for plasmid-based rescue. To increase the flexibility of AHSV-4 plasmid-based reverse genetics, we subsequently modified the 5-plasmid reverse genetics system by cloning a T7 RNA polymerase expression cassette, in which expression of the enzyme is under control of the constitutive cytomegalovirus (CMV) promoter, into the genetic backbone of the pJAD-S2-S6 reverse genetics vector. The derived plasmid was designated pJAD-S2-S6-T7pol and thus serves as a source of T7 RNA polymerase. Expression of the T7 RNA polymerase was confirmed by co-transfection of BSR cells with the pJAD-S2-S6-T7pol plasmid and a pJET-mKalama1 reporter plasmid, in which expression of the mKalama1 fluorescent protein is under transcriptional control of a T7 RNA polymerase promoter. Examination of the transfected cells at 16 h post-transfection by confocal microscopy indicated that, in contrast to mock-transfected cells, cells transfected with both plasmids fluoresced blue and thus confirmed expression of the plasmid-encoded T7 RNA polymerase (Supplementary Fig. S1).

To determine whether the modified 5-plasmid system allows recovery of AHSV-4, monolayers of BSR and L929 cells were co-transfected with the 5 plasmids encoding the AHSV-4 genome and T7 RNA polymerase (Fig. 5A). The cells were harvested at 3 days post-transfection, lysed and plaque assays were performed in BSR or L929 cells. In contrast to mock-transfected cells, plaques were recovered from the different cells transfected with the modified 5-plasmid set (Fig. 5B). At different time points post-transfection, viral titres in cell culture supernatants were also determined by plaque assays. The results showed that the titres of virus recovered following transfection of BSR and L929 cells with the modified 5-plasmid set increased over time, albeit that the titres of virus recovered in L929 cells were consistently lower than that in BSR cells (Fig. 5C). To confirm that AHSV-4 was indeed recovered following plasmid transfection, the recovered viruses were propagated in BSR and L929 cells, viral dsRNAs were extracted and analyzed by non-denaturing polyacrylamide gel electrophoresis. The profiles of viral dsRNAs from wild-type AHSV-4 as well as AHSV-4 recovered with the modified 5-plasmid system using BSR and L929 cells, were identical (Fig.

5D). Furthermore, both of the plasmid-derived AHSV-4 retained the *Pst*I restriction site in their S5 genome segments as a rescue-specific marker, thus confirming that the recovered AHSV-4 originated from plasmid DNA (data not shown). These results provide evidence that the modified 5-plasmid reverse genetics system can be used to recover AHSV-4 in cells that have not been engineered to express T7 RNA polymerase.

Recovery efficiencies of the different plasmid-based reverse genetics systems

To compare the efficiencies of AHSV-4 recovery between the 10-plasmid, 5-plasmid and modified 5-plasmid reverse genetics systems, monolayers of BSR-T7 or BSR cells were co-transfected with the appropriate plasmid sets as indicated above. The virus titres in the culture supernatant were determined at different time points post-transfection by plaque assay on BSR cells.

For each of the reverse genetics systems, the viral titre in the supernatant of transfected cells was below the limit of detection at 12 h post-transfection. However, the titre of recovered virus increased over time and maximal yields of virus were recovered at 5 days post-transfection, but significant yields were detected at 3 days post-transfection. The mean titres at days 3 and 5 post-transfection were approximately 51 and 2×10^2 pfu/ml, respectively, when BSR-T7 cells were transfected with the 10-plasmid system, whereas the virus yield using the 5-plasmid system determined at the same time points was approximately 4×10^2 and 3×10^3 pfu/ml, respectively. Virus yield was also high in the BSR cells co-transfected with the modified 5-plasmid system, with approximately 0.9×10^2 and 5×10^2 pfu/ml estimated at days 3 and 5 post-transfection, respectively (Fig. 6). From this data we conclude that AHSV-4 can be recovered using each of the developed reverse genetics systems and that reduction in plasmid number substantially improves rescue efficiency.

Discussion

Amongst the orbiviruses, bluetongue virus (BTV) has been studied the most extensively and thus serves as a model system for the distantly related AHSV. Despite similarities in their overall morphology, coding strategy and virus replication cycle, AHSV is, however, significantly different from BTV at both the genetic and structural levels and in the proteins it

encodes (Kaname et al., 2013). Moreover, AHSV causes disease in horses and its pathogenesis is different from that caused by BTV infections in sheep and cattle (Coetzer and Guthrie, 2004; MacLachlan et al., 2009). To address this imbalance, attempts have been made to study the structure-function relationships of individual AHSV proteins through a strategy of mutagenesis and re-expression of the proteins in heterologous hosts (Uitenweerde et al., 1995; Maree and Huismans, 1997; van Niekerk et al., 2001; de Waal and Huismans, 2005; Stassen et al., 2011; Bekker et al., 2014). However, a definitive role for many of these proteins in the context of a replicating virus remains unresolved. Consequently, the purpose of this study was to establish a reverse genetics system for the recovery of recombinant AHSV based entirely on cloned copies of the viral genome and, once established, to introduce improvements to the system that will expand the utility of reverse genetics for studies on AHSV biology.

During the development of reverse genetics systems for different RNA viruses, instability of cloned cDNA sequences in *Escherichia coli* have been reported for coronaviruses (Casais et al., 2000; Yount et al., 2000; Thiel et al., 2001), flaviviruses (Ward and Davidson, 2008; Pu et al., 2011) and influenza virus (Zhou et al., 2011). Likewise, we occasionally found that cDNA copies of selected AHSV-4 genome segments, especially S3, were prone to deletions and rearrangements when cloned into the previously constructed pRG15 reverse genetics plasmid and cultured in *E. coli*. Although the reasons for this phenomenon was not investigated, such instability of cloned DNA sequences may be caused by different factors, including long repeat sequences, secondary and tertiary structures, the presence of active *E. coli*-like promoter sequences within the insert and the generation of toxic proteins (Godiska et al., 2010; Pu et al., 2011). Based on previous reports indicating that the stability of inserts in circular vectors can be increased by the use of transcriptional terminators (Godiska et al., 2005; Zhou et al., 2011), we thus incorporated bidirectional T7Te terminators flanking the T7 RNA polymerase transcription cassettes present in the pJAD reverse genetics vectors. The successful cloning of cDNA copies of the AHSV-4 genome segments into the pJAD vectors and their stable maintenance using standard protocols suggest that that the backbone of these vectors may provide enhanced stability for unstable AHSV-4 virus genome segments.

The initial AHSV-4 reverse genetics system developed here consists of 10 plasmids, each containing a full-length cDNA copy of single AHSV-4 genome segments flanked by T7 RNA polymerase promoter and HDV ribozyme sequences. These plasmids are presumed to

generate 10 transcripts corresponding to native positive-sense RNAs that serve as templates for translation and dsRNA replication. The AHSV-4 replication cycle is initiated by transfection of the 10 plasmids encoding the viral genome into cells expressing T7 RNA polymerase. Using this system, we demonstrated production of AHSV-4 from the cloned cDNAs and showed that this 10-plasmid reverse genetics system permits the selective introduction of desired mutations into the viral genome without the need for a helper virus and selection system. The growth kinetics and genomic electrophoretic profiles were indistinguishable between plasmid-derived AHSV-4 and wild-type AHSV-4, indicating that the replication characteristics of the AHSV-4 generated from cloned cDNA reflect that of the wild-type AHSV-4.

It is interesting to note that contrary to current RNA-based reverse genetics systems that all depend on the use of capped synthetic transcripts (Boyce et al., 2008; Kaname et al., 2013; Vermaak et al., 2015; Yang et al., 2015), the RNAs transcribed *in situ* from the recombinant plasmids will not contain a 5' cap. These uncapped transcripts can nevertheless functionally substitute for viral transcripts at all stages of the AHSV replication cycle, as evidenced by the recovery of viable AHSV-4. These results are in agreement with those reported for reoviruses (Kobayashi et al., 2007; Kawagishi et al., 2016) and BTV (Pretorius et al., 2015). It is plausible that the sustained synthesis of RNA transcripts *in situ* results in sufficient levels of expression to allow the assembly of core particles, which themselves are transcriptionally active (Vermaak et al., 2015), and thus lead to an amplification of gene transcription.

A second aim of this study was to improve the performance of the developed AHSV-4 reverse genetics system by increasing the efficiency of virus recovery. To accomplish this aim, we reduced the number of plasmids required to deliver the entire AHSV-4 genome into BSR-T7 cells from 10 to 5 by combining two genome segment transcription cassettes into a single plasmid. Compared to the 10-plasmid reverse genetics system, this 5-plasmid strategy enhanced the efficiency of virus recovery by reducing the time to virus isolation and supporting increased total yields. The efficiency of virus recovery may have been enhanced by different mechanisms. Firstly, there are fewer plasmids that need to be transfected into each cell, and thus there is a higher probability that a full set of viral RNAs will accumulate in a cell for initiation of replication. Secondly, it is possible that only a small fraction of transfected plasmids avoid degradation and remain intact for transcription. By decreasing the number of plasmids the probability that a single cell will contain all of the transcription

cassettes in a sufficient number is enhanced. Thirdly, constriction of transcription and translation of individual RNAs to the same intracellular micro-environment may greatly facilitate protein-protein and protein-RNA interactions required for virus recovery (Neumann et al., 2005; Kobayashi et al., 2010). The 5-plasmid AHSV-4 reverse genetics system was sufficiently robust to allow the recovery of a directed cross-serotype reassortant virus.

Technical complexities associated with the construction and manipulation of the dual reverse genetics plasmids may make their use less appealing. In this regard, the 10-plasmid reverse genetics system remains a useful alternative for demanding cloning tasks. For example, we generated the $_{A4}$AHSV-1$^{VP2/VP5}$ reassortant virus by combining four AHSV-4 dual plasmids and a dual plasmid containing cDNA copies of the S2 and S6 genome segments from AHSV-1. However, the same reassortant virus was also recovered successfully by combining the four AHSV-4 dual vectors with two single reverse genetics plasmids, which contained cDNA copies of the S5 and S6 genome segments, respectively. The efficiency of virus recovery was slightly lower compared to the use of 5 dual plasmids and is likely due to a lower transfection efficiency associated with the requirement for an additional plasmid for transection (data not shown). Such an approach may be useful to generate so-called "serotyped" vaccine strains in which the immunogenic outer capsid proteins are exchanged with those of other virus serotypes (van Gennip et al., 2012; Feenstra et al., 2014; Feenstra et al., 2015; van de Water et al., 2015). Thus, the single reverse genetics plasmids remain important adjuncts to the 5-plasmid reverse genetics system by enhancing flexibility with gains in efficiency.

Although both the 10- and 5-plasmid reverse genetics systems are sufficient for generating recombinant AHSV-4, it would be an advantage if the dependence of virus recovery on the use of BSR-T7 cells could be overcome. To this end, we have cloned a T7 RNA polymerase expression cassette onto the genetic backbone of the pJAD-S2-S6 dual reverse vector and subsequently demonstrated that AHSV-4 could be recovered in BSR and L929 cells following transfection of the cells with the modified 5-plasmid set. In these experiments, the titre of AHSV-4 recovered in L929 cells was lower than that of virus recovered in BSR cells. This difference in virus titres may be ascribed to the ability of L929 cells to produce interferons (Takano-Maruyama et al., 2006), whereas BSR and BSR-T7 cells lack an interferon response (Rieder et al., 2011). These findings nevertheless provide evidence that this alternative 5-plasmid reverse genetics system can be employed using cell lines that have

not been engineered to express T7 RNA polymerase, and thus provides for a streamlined reverse genetics system for recovery of AHSV-4 in different cell lines.

In conclusion, we have established a basic reverse genetics system for AHSV-4 and made improvements to the system that increase the flexibility and efficiency of reverse genetics, and also allows for the recovery of AHSV-4 in cells that have not been engineered to express T7 RNA polymerase. These entirely plasmid-based reverse genetics systems opens new possibilities for investigating virus infection at the molecular level, including virus protein function, virus replication, host-virus-vector interactions and pathogenesis. Moreover, the ability to recover mutant and reassortant viruses indicates that these reverse genetics systems can be exploited to generate further recombinant viruses that could be potential live-attenuated vaccines.

Materials and Methods

Cells and viruses

BSR cells (a clone of baby hamster kidney-21 cells) were cultured in Eagle's minimum essential medium (EMEM) supplemented with Earle's balanced salt solution (EBSS), 2 mM L-glutamine, 5% (v/v) foetal bovine serum (FBS), 1% (v/v) non-essential amino acids (NEAA), and antibiotics (10 000 U/ml of penicillin, 10 000 µg/ml of streptomycin, 25 µg/ml of amphotericin B) (Hyclone). L929 (mouse fibroblast) cells were cultured in Dulbecco's modified Eagle's medium (DMEM) supplemented with 5% (v/v) FBS and antibiotics (100 U/ml of penicillin, 100 µg/ml of streptomycin) (Gibco). BSR-T7 cells, which stably express bacteriophage T7 RNA polymerase (Buchholtz et al., 1999), were maintained in the same manner as BSR cells, except for the addition of 1 mg/ml of Geneticin (Invitrogen) with every second passage of the BSR-T7 cells. All mammalian cell lines were grown at 37°C with 5% CO_2.

AHSV serotypes 1 (AHSV-1) and 4 (AHSV-4) were used in this study. The origin of AHSV-4 has been described previously (van de Water et al., 2015) and is a live-attenuated vaccine strain (AHSV-4LP) that was obtained by attenuation of virulent AHSV HS32/62 through passage in suckling mice and BHK-21 cells, followed by selection of large plaques on Vero cells (Erasmus, 1972). For cell infections, BSR cell monolayers were rinsed twice with incomplete EMEM (lacking FBS and antibiotics) and then infected with virus at a

multiplicity of infection (MOI) of 0.1 pfu/cell. Virus adsorptions were performed at 37°C for 1 h, followed by incubation of the cell monolayers in complete EMEM for 72 h.

Construction of pJAD1 and pJAD2 reverse genetics vectors

The pJAD1 and pJAD2 reverse genetics vectors share the same pUC19 genetic backbone, which lacks the *lacZ*' region inclusive of the multiple cloning site, and was prepared by an inverse PCR using pUC19 as template (GenBank accession no. M77789.2) together with primers iPCR-F and iPCR-R (Table 1). To construct pJAD1, a transcription cassette comprising a T7 RNA polymerase promoter, followed by two inverted *Bsm*BI restriction enzyme sites, a hepatitis delta virus (HDV) ribozyme sequence and a T7 RNA polymerase terminator sequence, was PCR-amplified from plasmid pRG15 (Pretorius et al., 2015) using primers Cas1F and Cas1R (Table 1). The amplicon was phosphorylated using T4 Polynucleotide kinase (Thermo Scientific) and then blunt-end ligated to the modified pUC19 genetic backbone. A similar strategy was used to construct pJAD2, except that the transcription cassette was PCR-amplified from plasmid pRG15 with primers Cas2F and Cas2R (Table 1). The nucleotide sequence of the cloned insert DNAs was verified by automated sequencing procedures using the ABI PRISM BigDye Terminator Cycle Sequencing Ready Reaction kit v3.1 (Perkin-Elmer Applied Biosystems). The pJAD1 and pJAD2 reverse genetics vectors thus harbour identical transcription cassettes flanked by bidirectional T7Te terminators (Reynolds et al., 1992a; Reynolds et al., 1992b) and contain unique restriction enzyme sites (*Stu*I and/or *Pme*I) to facilitate cloning procedures (Fig. 1).

Cloning of AHSV-4 cDNA into pJAD1 and pJAD2

Total RNA was extracted from BSR cells infected with AHSV-4 using the Nucleospin RNA II kit (Macherey-Nagel) and ssRNA was removed by precipitation with 2 M LiCl and centrifugation at 17 000 *g* for 30 min at 4°C. First-strand cDNA was synthesized from 3 µg of dsRNA using the RevertAid H Minus First Strand cDNA Synthesis kit (Thermo Scientific), and cDNA copies of the full-length AHSV-4 genome segments were amplified by PCR using genome segment-specific primer pairs (Table 1) and high-fidelity Velocity DNA polymerase (Bioline). The purified amplicons were phosphorylated and then blunt end-ligated to the respective pJAD vectors that had been linearized by means of an inverse PCR using primers InvF and InvR (Table 1). These back-to-back primers were designed to flank

the poorly digestible *BsmB*I cloning site present in the pJAD vectors and thus resulted in the amplification of the vector DNA excepting the cloning site between the two primers. cDNA copies of AHSV-4 genome segments S1 through S5 were ligated to the pJAD1 vector, and cDNA copies of genome segments S6 through S10 were ligated to the pJAD2 vector to generate pJAD-S1 through pJAD-S10. The sizes of the recombinant plasmids are provided in Supplementary Table S1. Plasmid pJAD-S5, encoding the entire AHSV-4 S5 genome segment, has a *Pst*I restriction site as a genetic marker that was created by introducing a single nucleotide change at position 1010 in the S5 genome segment using the QuickChange Site-Directed Mutagenesis kit (Stratagene) and primers S5PstI-F and S5PstI-R (Table 1). The nucleotide sequence and transcriptional orientation of cloned cDNA was verified by automated sequencing procedures. With the exception of the single nucleotide substitution introduced into the S5 genome segment cDNA, the sequences exactly matched the database sequences (GenBank accession nos. KM820849 to KM820858; Potgieter et al., 2009; van de Water et al., 2015).

Construction of consolidated AHSV-4 reverse genetics plasmids

Recombinant AHSV-4 generation from five plasmids was facilitated by combining two genome segment transcription cassettes flanked by T7Te terminators onto one plasmid. To this end, recombinant plasmids pJAD-S6 through pJAD-S10 were digested with *Pme*I, and the excised DNA fragments were blunt-end cloned into the *Pme*I site of pJAD-S1 through pJAD-5. The derived reverse genetics plasmids were named pJAD-S1-S8, pJAD-S2-S6, pJAD-S3-S7, pJAD-S4-S10 and pJAD-S5-S9 (Supplementary Table S1). The integrity of the recombinant plasmids was verified by nucleotide sequencing of the genome segment transcription cassettes present in each of the recombinant constructs.

Construction of pJAD-S2-S6-T7pol

To enable the recovery of recombinant AHSV-4 from plasmid DNA in cell lines that have not been engineered to express T7 RNA polymerase (GenBank Accession no. AM946981), an expression cassette encoding for T7 RNA polymerase was incorporated into the genetic backbone of the pJAD-S2-S6 rescue plasmid. The coding region of the T7 RNA polymerase gene was PCR-amplified with Phusion High-Fidelity DNA polymerase (Thermo Scientific) using chromosomal DNA from *E. coli* BL21(DE3) as template and primers T7Bam-F and

T7Bam-R (Table 1), which both harbour a *Bam*HI site. The purified amplicon was digested with *Bam*HI and cloned into the *Bam*HI site of the pcDNA3.1(+) mammalian expression vector (Invitrogen) to generate pcDNA-T7pol. The recombinant plasmid DNA was characterized by nucleotide sequencing to confirm that the insert DNA was cloned under transcriptional control of the cytomegalovirus (CMV) immediate-early promoter. Subsequently, pcDNA-T7pol was used as template together with primers CMV-F and CMV-R (Table 1), both of which harbour an *Eco*RV site, to PCR amplify the T7 RNA polymerase expression cassette. This cassette comprised the T7 RNA polymerase coding region flanked by the upstream CMV promoter sequence and the downstream bovine growth hormone poly(A) sequence. The amplicon was digested with *Eco*RV and blunt-end cloned into the *Ssp*I site of plasmid pJAD-S2-S6 to yield pJAD-S2-S6-T7pol. The integrity of the cloned insert was verified by nucleotide sequencing.

Construction of plasmids for use in reassortant experiments

Using similar approaches to those described above, full-length cDNAs of AHSV-1 genome segments S2 and S6 were amplified by RT-PCR using viral dsRNA extracted from virus-infected cells as template. Segment-specific cDNAs were amplified by using primers 2.1F and 2.1R for S2, and primers 6.1F and 6.1R for S6 (Table 1). The amplified cDNA for the AHSV-1 S2 and S6 genome segments were cloned into pJAD1 and pJAD2, respectively, and the derived recombinant plasmids were designated pJAD(A1)-S2 and pJAD(A1)-S6. The integrity of the cloned cDNA in each of the plasmids was confirmed by nucleotide sequencing. The S6 genome segment transcription cassette flanked by T7Te terminators was recovered from pJAD(A1)-S6 by digestion with *Pme*I and cloned into *Pme*I-digested pJAD(A1)-S2 to generate plasmid pJAD(A1)-S2-S6.

Recovery of recombinant viruses from cloned cDNA

Plasmid DNA used in cell transfections was purified using the Genopure Plasmid Maxi kit (Roche Life Science) according to the manufacturer's instructions. Monolayers of BSR-T7 cells at 70% confluency in 6-well tissue culture plates were co-transfected with plasmids representing the cloned AHSV-4 genome using *Trans*IT-LT1 Transfection Reagent (Mirus). Briefly, 7.5 µl of the transfection reagent was added to 250 µl of OptiMEM I Reduced Serum Medium (Life Technologies) and incubated at room temperature for 30 min. For co-

transfection of the cells with the 10 recombinant pJAD plasmids, 250 ng of each plasmid was mixed in an Eppendorf tube and the plasmid DNA mixture was then added to the diluted transfection reagent. Following incubation at room temperature for 1 h, the transfection mixture was added to the BSR-T7 cells and OptiMEM I Reduced Serum Medium was added to a final volume of 3 ml. At 16 h post-incubation, the medium was replaced with complete EMEM. An identical protocol to that above was followed to recover recombinant AHSV-4 from BSR-T7 cells transfected with the 5-plasmid set, except that 500 ng of each plasmid was used. The same protocol was followed to generate a reassortant virus, except that the pJAD-S2-S6 plasmid was substituted with the pJAD(A1)-S2-S6 plasmid prior to transfection of the BSR-T7 cell monolayer. Recombinant AHSV-4 was likewise recovered in monolayers of BSR and L929 cells using the modified 5-plasmid reverse genetics system, except that BSR or L929 cells were co-transfected with 500 ng of each dual (pJAD-S1-S8, pJAD-S3-S7, pJAD-S4-S10 and pJAD-S5-S9) plasmid and 1 µg of the pJAD-S2-S6-T7pol plasmid, and the volume of the transfection reagent used was adjusted to 9 µl. Following 1 to 5 days of incubation, cells and medium were harvested, lysed and used in a plaque assay on BSR cells (Oellermann et al., 1970).

Characterization of plasmid-derived viruses

Viral dsRNAs were extracted from infected cells, electrophoresed on non-denaturing 10% polyacrylamide gels and visualized by ethidium bromide staining. To discriminate between wild-type and plasmid-derived AHSV-4, full-length cDNA products of genome segment S5 from recovered viruses were digested with *Pst*I and the digestion products were resolved by electrophoresis on a 1% agarose gel. As a final confirmation, the nucleotide sequence of the amplified S5 genome segments was also determined. To characterize reassortant viruses, cDNA was synthesized from the viral dsRNA and PCR amplification was performed using S2 and S6 genome segment-specific primer pairs for AHSV-1. The purified genome segment S6 PCR product was analyzed by agarose gel electrophoresis following digestion with *Bam*HI, and the nucleotide sequences of the S2 and S6 PCR products were also determined.

Growth kinetics

Confluent BSR cell monolayers in 6-well tissue culture plates were infected with either wild-type AHSV-4 or plasmid-derived AHSV-4 at a MOI of 0.1 pfu/cell. Virus adsorptions were

performed at 37°C for 1 h, after which the medium with unbound virus was removed. The monolayers were washed once with serum-free EMEM, 2 ml of complete EMEM was added and incubation was continued. At different time intervals post-infection the cells and medium were harvested. The samples were passed through a 22G needle and subjected to low-speed centrifugation to pellet cell debris. The virus titres were subsequently determined by serial dilution and plaque assays on BSR cells.

Comparison of AHSV-4 recovery using different reverse genetics systems

Monolayers of BSR-T7 cells were co-transfected with the 10-plasmid or 5-plasmid reverse genetics constructs and BSR cells were co-transfected with the modified 5-plamsid set, as described above. Aliquots (1 ml) of the supernatant of transfected cells were collected and replaced with 1 ml fresh medium at 12 h, 3 days and 5 days post-transfection. Virus titres in the culture supernatants were determined by plaque assays on BSR cells.

Confocal microscopy

To confirm expression of the plasmid-encoded T7 RNA polymerase, BSR cell monolayers, grown on sterile glass coverslips in 6-well tissue culture plates, were co-transfected with pJAD-S2-S6-T7pol (2 µg) and the reporter plasmid pJET-mKalama1 (800 ng) sing *Trans*IT-LT1 Transfection Reagent (Mirus). In the reporter plasmid, the coding region of mKalama1 is under transcriptional control of a T7 RNA polymerase promoter. At 16 h post-transfection, the glass coverslips were removed and mounted onto glass slides, which were viewed with a Zeiss LSM S10 Meta confocal microscope. The images were captured with a Zeiss Axiovert Series 5 digital camera and analyzed with Zeiss LSM Image Browser v.4.2.0.121.

Acknowledgments

This work was supported by the University of Pretoria's Institutional Research Theme Programme (Grant AOU999), Poliomyelitis Research Foundation (Grant 13/19) and the Technology Innovation Agency (Grant TAHC12-00028). Graduate bursary (AMC) and postdoctoral fellowship (LS) support was received from the National Research Foundation and the Poliomyelitis Research Foundation.

References

Alberca, B., Bachanek-Bankowska, K., Cabana, M., Calvo-Pinilla, E., Viaplana, E., Frost, L., Gubbins, S., Urniza, A., Mertens, P., Castillo-Olivares, J., 2014. Vaccination of horses with a recombinant modified vaccinia Ankara virus (MVA) expressing African horse sickness (AHS) virus major capsid protein VP2 provides complete clinical protection against challenge. Vaccine 32, 3670-3674.

Bekker, S., Huismans, H., van Staden, V., 2014. Factors that affect the intracellular localization and trafficking of African horse sickness virus core protein, VP7. Virology 456-457, 279-291.

Boyce, M., Celma, C.C.P., Roy, P., 2008. Development of reverse genetics systems for bluetongue virus: Recovery of infectious virus from synthetic RNA transcripts. J. Virol. 82, 8339-8348.

Bremer, C.W., Huismans, H., van Dijk, A.A., 1990. Characterization and cloning of the African horsesickness virus genome. J. Gen. Virol. 71, 793-799.

Buchholz, U.J., Finke, S., Conzelmann, K-K., 1999. Generation of bovine respiratory syncytial virus (BRSV) from cDNA: BRSV NS2 is not essential for virus replication in tissue culture, and the human RSV leader region acts as a functional BRSV genome promoter. J. Virol. 73, 251-259.

Casais, R., Volker, T., Siddell, S.G., Cavanagh, D., Britton, P., 2001. Reverse genetics system for the avian coronavirus infectious bronchitis virus. J. Virol. 24, 12359-12369.

Clift, S.J., Penrith, M.L., 2010. Tissue and cell tropism of African horse sickness virus demonstrated by immunoperoxidase labeling in natural and experimental infection in horses in South Africa. Vet. Path. 47, 690-697.

Coetzer, J.A.W., Guthrie, A., 2004. African horse sickness. In: Infectious Diseases of Livestock. Second edition. Coetzer, J.A.W., Tustin, R.C. (Eds.). Oxford University Press, South Africa, pp. 1231-1246.

de Waal, P.J., Huismans, H., 2005. Characterization of the nucleic acid binding activity of inner core protein VP6 of African horse sickness virus. Arch. Virol. 150, 2037-2050.

Dermody, T.S., Parker, J.S.L., Sherry, B., 2013. Orthoreoviruses. In: Fields Virology. Sixth edition. Knipe, D.M., Howley, P.M. (Eds.). Lippincott & Wilkins, Philadelphia, pp. 1304-1346.

Diaz Montilla, R., Panos Marti, P., 1967. Epidemiology of AHS in Spain. Bull. Off. Int. Epizoot. 68, 705-714.

Erasmus, B.J., 1972. The pathogenesis of African horse sickness. In: Proceedings of the Third International Conference on Equine Infectious Diseases. Karger, Basel, Switzerland, pp. 1-11.

Feenstra, F., Maris-Veldhuis, M., Daus, F.J., Tacken, M.G., Moormann, R.J., van Gennip, R.G., van Rijn, P.A., 2014. VP2-serotyped live-attenuated bluetongue virus without NS3/NS3a expression provides serotype-specific protection and enables DIVA. Vaccine 32, 7108-7114.

Feenstra, F., Pap, J.S., van Rijn, P.A., 2015. Application of bluetongue disabled infectious single animal (DISA) vaccine for different serotypes by VP2 exchange or incorporation of chimeric VP2. Vaccine 33, 812-818.

Forzan, M., Marsh, M., Roy, P., 2007. Bluetongue virus entry into cells. J. Virol. 81, 4819-4827.

Godiska, R., 2005. Beyond pUC: Vectors for cloning unstable DNA. In: DNA Sequencing: Optimizing the Process and Analysis. Volume 1, First Edition. Kieleczawa, J. (Ed.). Jones and Bartlett Publishers, Massachusetts, pp. 55-76.

Godiska, R., Mead, D., Dhodda, V., Wu, C., Hochstein, R., Karsi, A., Usdin, K., Entezam, A., Ravin, N., 2010. Linear plasmid vector for cloning of repetitive or unstable sequences in *Escherichia coli*. Nucl. Acids Res. 38(6), e88.

Guthrie, A.J., 2007. African horse sickness. In: Equine Infectious Diseases. Sellon, D.C., Long, M.T. (Eds.). Saunders Elsevier, St Louis, pp. 164-171.

Guthrie, A.J., Quana, M., Lourensa, C.W., Audonnet, J., Minkeb, J.M., Yao, J., He, L., Nordgren, R., Gardner, I.A., MacLachlan, N.J., 2009. Protective immunization of horses with a recombinant canary pox virus vectored vaccine co-expressing genes encoding the outer capsid proteins of African horse sickness virus. Vaccine 16, 4434-4438.

Howell, P.G., 1960. The 1960 epizootic of African horsesickness in the Middle East and SW Asia. J. South Afr. Vet. Assoc. 31, 329-335.

Kaname, Y., Celma, C.C., Kanai, Y., Roy, P., 2013. Recovery of African horse sickness virus from synthetic RNA. J. Gen. Virol. 94, 2259-2265.

Kawagishi, T., Kanai, Y., Tani, H., Shimojima, M., Saijo, M., Matsuura, Y., Kobayashi, T., 2016. Reverse genetics for fusogenic bat-borne orthoreovirus associated with acute respiratory tract infections in humans: Role of outer capsid protein σC in viral replication and pathogenesis. PLoS Pathog. 12, e1005455.

Kobayashi, T., Antar, A.A.R., Boehme, K.W., Danthi, P., Eby, E.A., Guglielmi, K.M., Holm, G.H., Johnson, E.M., Maginnis, M.S., Naik, S., Skelton, W.B., Wetzel, J.D., Wilson, G.J., Chappell, J.D., Dermody, T.S., 2007. Plasmid-based reverse genetics for animal double-stranded RNA viruses. Cell Host Microbe 1, 147-157.

Kobayashi, T., Ooms, L.S., Ikizler, M., Chappel, J.D., Dermody, T.S., 2010. An improved reverse genetics system for mammalian orthoreoviruses. Virology 398, 194-200.

Komoto, S., Sasaki, J., Taniguchi, K., 2006. Reverse genetics system for introduction of site-specific mutations into the double-stranded RNA genome of infectious rotavirus. Proc. Natl. Acad. Sci USA 103, 4646-4651.

Komoto, S., Taniguchi, K., 2013. Genetic engineering of rotaviruses by reverse genetics. Microbiol. Immunol. 57, 479-486.

Lubroth, J., 1988. African horsesickness and the epizootic in Spain 1987. Equine Pract. 10, 26-33.

MacLachlan, N.J., Guthrie, A., 2010. Re-emergence of bluetongue, African horse sickness, and other orbivirus diseases. Vet. Res. 41, 35-47.

MacLachlan, N.J., Drew, C.P., Darpel, K.E., Worwa, G., 2009. The pathology and pathogenesis of Bluetongue. J. Comp. Path. 141, 1-16.

Manole, V., Laurinmäki, P., van Wyngaardt, W., Potgieter, C.A., Wright, I.M., Venter, G.J., van Dijk, A.A., Sewell, B.T., Butcher, S.J., 2012. Structural insight into African horsesickness virus infection. J. Virol. 86, 7858-7866.

Maree, F.F., Huismans, H., 1997. Characterization of tubular structures composed of nonstructural protein NS1 of African horsesickness virus expressed in insect cells. J. Gen. Virol. 78, 1077-1082.

Martinez-Lopez, B., Perez, A.M., Sanchez-Vizcaino, J.M., 2011. Identifying equine premises at high risk of introduction of vector-borne diseases using geo-statistical and space-time analyses. Prev. Vet. Med. 15, 100-108.

Matsuo, E., Roy, P., 2013. Minimum requirements for bluetongue virus primary replication *in vivo*. J. Virol. 87, 882-889.

Mellor, P.S., Boorman, J., Baylis, M., 2000. *Culicoide*s biting midges: Their role as arbovirus vectors. Annu. Rev. Entomol. 45, 307-340.

Mertens, P.P., Diprose, J., 2004. The bluetongue virus core: A nano-scale transcription machine. Virus Res. 101, 29-43.

Neumann, G., Fuji, K., Kino, Y., Kawaoka, Y., 2005. An improved reverse genetics system for influenza A virus generation and its implications for vaccine production. Proc. Natl. Acad. Sci. USA 102, 16825-16829.

Oellermann, R.A., 1970. Plaque formation by African horsesickness virus and characterisation of its RNA. Onderstepoort J. Vet. Res. 37, 137-144.

Patel, A., Roy, P., 2014. The molecular biology of bluetongue replication. Virus Res. 182, 5-20.

Portas, M., Boinas, F.S., Oliveira, E.S.J., Rawlings, P., 1999. African horse sickness in Portugal: A successful eradication programme. Epidemiol. Infect. 123, 337-346.

Potgieter, A.C., Page, N.A., Liebenberg, J., Wright, I.M., Landt, O., van Dijk, A.A., 2009. Improved strategies for sequence-independent amplification and sequencing of viral double-stranded RNA genomes. J. Gen. Virol. 90, 1423-1432.

Pretorius, J.M., Huismans, H., Theron, J., 2015. Establishment of an entirely plasmid-based reverse genetics system for bluetongue virus. Virology 486, 71-77.

Pu, S-Y., Wu, R-H., Yang, C-C., Jao, T-M., Tsai, M-H., Wang, J-C., Lin, H-M., Chao, Y-S., Yueh, A., 2011. Successful propagation of flavivirus infectious cDNAs by a novel method to reduce the cryptic bacterial promoter activity of virus genomes. J. Virol. 85, 2927-2941.

Purse, B.V., Brown, H.E., Harrup, L., Mertens, P.P.C., Rogers, D.J., 2008. Invasion of bluetongue and other orbivirus infections into Europe: The role of biological and climatic processes. Rev. Sci. Tech. OIE 27, 427-442.

Rafyi, A., 1961. Horse sickness. Bull. Off. Int. Epizoot. 56, 216-250.

Reynolds, R., Bermudez, M., Chamberlin, M.J., 1992a. Parameters affecting transcription termination by *Escherichia coli* RNA polymerase: I. Analysis of 13 Rho-independent terminators. J. Mol. Biol. 224, 31-51.

Reynolds, R., Chamberlin, M.J., 1992b. Parameters affecting transcription termination by *Escherichia coli* RNA. II. Construction and analysis of hybrid terminators. J. Mol. Biol. 224, 53-63.

Rieder, M., Brzózka, K., Pfaller, C.K., Cox, J.H., Stitz, L., Conzelmann, K-H. (2011). Genetic dissection of interferon-antagonistic functions of rabies virus phosphoprotein: Inhibition of interferon regulatory factor 3 activation is important for pathogenicity. J. Virol. 85, 842-852.

Rodriguez, M., Hooghuis, H., Castano, M., 1992. African horse sickness in Spain. Vet. Microbiol. 33, 129-142.

Roy, P., 2013. Orbiviruses. In: Fields Virology. Sixth edition. Knipe, D.M., Howley, P.M. (Eds.). Lippincott & Wilkins, Philadelphia, pp. 1402-1423.

Scanlen, M., Paweska, J.T., Verschoor, J.A., van Dijk, A.A., 2002. The protective efficacy of a recombinant VP2-based African horsesickness subunit vaccine candidate is determined by adjuvant. Vaccine 20, 1079-1088.

Stassen, L., Huismans, H., Theron, J., 2011. Membrane permeabilization of the African horse sickness virus VP5 protein is mediated by two N-terminal amphipathic α-helices. Arch. Virol. 156, 711-715.

Stassen, L., Vermaak, E., Theron, J., 2014. African horse sickness, an equine disease of emerging global significance. In: Horses: Breeding, Health Disorders and Effects on Performance and Behaviour. Paz-Silva, A., Sol Arias Vázquez, M., Sánchez-Andrade Fernández, R. (Eds.). Nova Science Publishers, Inc., New York, pp. 145-170.

Tabachnick, W.J., 2010. Challenges in predicting climate and environmental effects on vector-borne disease episystems in a changing world. J. Exp. Biol. 213, 946-954.

Takano-Maruyama, M., Ohara, Y., Asakura, K., Okuwa, T., 2006. Theiler's murine encephalomyelitis virus leader protein amino acid residue 57 regulates subgroup-specific virus growth on BHK-21 cells. J. Virol. 80, 12025-12031.

Thiel, V., Herold, J., Schelle, B., Siddell, S.G., 2001. Infectious RNA transcribed *in vitro* from a cDNA copy of the human coronavirus genome cloned in vaccinia virus. J. Gen. Virol. 82, 1273-1281.

Trask, S.D., Boehme, K.W., Dermody, T.S., Patton, J.T., 2013. Comparative analysis of *Reoviridae* reverse genetics methods. Methods 59, 199-206.

Trask, S.D., Taraporewala, Z.F., Boehme, K.W., Dermody, T.S., Patton, J.T., 2010. Dual selection mechanisms drive efficient single-gene reverse genetics for rotavirus. Proc. Natl. Acad. Sci. USA 107, 18652-18657.

Troupin, C., Dehee, A., Schnuriger, A., Vende, P., Poncet, D., Garbarg-Chenon, A., 2010. Rearranged genomic RNA segments offer a new approach to the reverse genetics of rotaviruses. J. Virol. 84, 6711-6719.

Uitenweerde, J.M., Theron, J., Stoltz, M.A., Huismans, H., 1995. The multimeric nonstructural NS2 proteins of Bluetongue virus, African horsesickness virus, and Epizootic haemorrhagic disease virus differ in their single-stranded RNA-binding ability. Virology 209, 624-632.

van de Water, S.G.P., van Gennip, R.G.P., Potgieter, C.A., Wright, I.M., van Rijn, P.A., 2015. VP2 exchange and NS3/NS3a deletion in African horse sickness virus (AHSV) in development of disabled infectious single animal vaccine candidates for AHSV. J. Virol. 89, 8764-8772.

van Gennip, R.G., van de Water, S.G., Maris-Veldhuis, M., van Rijn, P.A., 2012. Bluetongue viruses based on modified-live vaccine serotype 6 with exchanged outer shell proteins confer full protection in sheep against virulent BTV8. PLoS One 7, e44619.

van Niekerk, M., Smit, C.C., Fick, W.C., van Staden, V., Huismans, H., 2001. Membrane association of African horsesickness virus nonstructural protein NS3 determines its cytotoxicity. Virology 279, 499-508.

van Staden, V., Stoltz, M.A., Huismans, H., 1995. Expression of non-structural protein NS3 of African horsesickness virus (AHSV): Evidence for a cytotoxic effect of NS3 in insect cells, and characterization of the gene products in AHSV-infected Vero cells. Arch. Virol. 140, 289-306.

Venter, G.J., Wright, I.M., Van Der Linde, T.C., Paweska, J.T., 2009. The oral susceptibility of South African field populations of *Culicoides* to African horse sickness virus. Med. Vet. Entomol. 23, 367-378.

Vermaak, E., Paterson, D.J., Conradie, A., Theron, J., 2015. Directed genetic modification of African horse sickness virus by reverse genetics. S. Afr. J. Sci. 111(7/8), Art. 2014-0331.

Ward, R., Davidson, A.D., 2008. Reverse genetics and the study of dengue virus. Future Virol. 3, 279-290.

Yang, T., Zhang, J., Xu, Q., Sun, E., Li, J., Lv, S., Feng, Y., Zhang, Q., Wang, H., Wang, H., Wu, D., 2015. Development of a reverse genetics system for epizootic haemorrhagic disease virus and evaluation of novel strains containing duplicative gene rearrangements. J. Gen. Virol. 96, 2714-2720.

Yount, B., Curtis, K.M., Baric, R.S., 2000. Strategy for systematic assembly of large RNA and DNA genomes: Transmissible gastroenteritis virus model. J. Virol. 74, 10600-10611.

Zhang, X., Kong, W., Ashraf, S., Curtiss, R., 2011. A one-plasmid system to generate influenza virus in cultured chicken cells for potential use in influenza vaccine. J. Virol. 83, 9296-9303.

Zhou, B., Jerzak, G., Scholes, D.T., Donnelly, M.E., Li, Y., Wentworth, D.E., 2011. Reverse genetics plasmid for cloning unstable influenza A virus gene segments. J. Virol. Meth. 173, 378-383.

Zwart, L., Potgieter, C.A., Clift, S.J., van Staden, V., 2015. Characterising non-structural protein NS4 of African horse sickness virus. PLoS One 10, e0124281.

Figure legends

Fig. 1. Plasmid maps of the pJAD1 and pJAD2 reverse genetics vectors. In each of the pJAD1 and pJAD2 vectors (A), cloned cDNAs of the 10 full-length AHSV-4 dsRNA genome segments are flanked by a bacteriophage T7 RNA polymerase promoter and a HDV ribozyme sequence (B). Since the T7 RNA polymerase promoter directs transcription initiation from a juxtaposed guanosine residue and considering that all AHSV positive-sense RNAs are terminated with a guanosine, plasmid-generated transcripts are thus anticipated to possess the native 5'-end. Autocatalytic cleave of the nascent transcripts generates the native viral 3'-end. The transcription cassette in each reverse genetics vector is flanked by bidirectional T7Te terminators and restriction enzyme sites to facilitate cloning procedures are indicated.

Fig. 2. Recovery of AHSV-4 from cDNA plasmids only. (A) Schematic of the approach. The 10 AHSV-4 constructs are co-transfected into BSR-T7 cells. Cytoplasmic transcription of the cloned cDNAs yield transcripts corresponding to viral positive-sense mRNAs with native 5' and 3' termini. Following 3-5 days of incubation, transfected cells are lysed and viable viruses are isolated by plaque assays on BSR cells. (B) Plaque assays of transfection cell lysates performed 5 days post-transfection (well 2). Mock-transfected cells were included as a control (well 1). (C) Electropherotypes of wild-type (WT) and plasmid-derived AHSV-4 (lanes 1 and 2). BSR cells were infected with wild-type AHSV-4 or rescued AHSV-4. At 72 h post-infection the viral dsRNA was extracted and electrophoresed in a non-denaturing polyacrylamide gel, followed by staining with ethidium bromide to visualize viral genome segments (S1-S10). (D) Digestion of the S5 genome segment RT-PCR products of wild-type AHSV-4 (WT) and plasmid-derived AHSV-4 (lanes 1 and 2) with *Pst*I to confirm the presence of a novel mutation introduced into the S5 genome segment of plasmid-derived viruses. Size markers (M) are indicated in base pairs. The nucleotide sequence of the RT-PCR products was also determined and compared. Shown is the sequence chromatogram demonstrating the A→G substitution at nucleotide 1010 that creates a novel *Pst*I restriction site in the S5 genome segment of recombinant AHSV-4. (E) Growth kinetics of wild-type (wt) AHSV-4 and plasmid-derived AHSV-4 (rAHSV-4) in BSR cells. Cells were infected with virus at a MOI of 0.1 pfu/ml and incubated for the intervals shown. Virus titres in cell lysates were determined by plaque assays on BSR cells. The results are presented as the mean virus titres of three independent experiments and error bars indicate the standard deviation.

Fig. 3. Improved plasmid-based reverse genetics system for AHSV-4. (A) Two genome segment transcription cassettes encoding AHSV-4 cDNA flanked by the T7 RNA polymerase promoter and HDV ribozyme sequences were combined into a single plasmid, creating 5 plasmids encoding the viral genome. The procedure for AHSV-4 recovery is near identical to that for the 10-plasmid system, except that BSR-T7 cells are co-transfected with the 5 plasmids. (B) Plaque assays of transfection cell lysates performed 3 days post-transfection (well 2). Mock-transfected cells were included as a control (well 1). (C) Electropherotypes of wild-type (WT) and plasmid-derived AHSV-4 (lanes 1 and 2). The viral dsRNA was extracted from infected BSR cells at 72 h post-infection, separated on a non-denaturing polyacrylamide gel and visualized by staining with ethidium bromide. The genome segments (S1-S10) are indicated. (D) Digestion of the S5 genome segment RT-PCR products of wild-type AHSV-4 (WT) and plasmid-derived AHSV-4 (lanes 1 and 2) using *Pst*I to confirm the presence of the signature mutation in the S5 genome segment as a genetic marker for viruses rescued from plasmid cDNA. Size markers (M) in base pairs are indicated.

Fig. 4. Characterization of the reassortant virus $_{A4}$AHSV-1$^{VP2/VP5}$. (A) Electropherotype of the reassortant virus $_{A4}$AHSV-1$^{VP2/VP5}$ (lane 1) obtained by electrophoresis of the genomic dsRNA in a non-denaturing polyacrylamide gel, followed by ethidium bromide staining to visualize viral genome segments (S1-S10). The reassortant virus contains genome segments S2 and S6 from AHSV-1 in an otherwise AHSV-4 genetic background. Wild-type AHSV-4 dsRNA (A-4) and AHSV-1 dsRNA (A-1) marker lanes are indicated to the left and right of the figure, respectively. The asterisk indicates the faster migrating S2 genome segment of AHSV-1, whereas the origin of the S6 genome segment was determined by restriction enzyme digestion. (B) Restriction digestion analysis of genome segment S6 RT-PCR products from AHSV-4, AHSV-1 and the reassortant virus $_{A4}$AHSV-1$^{VP2/VP5}$. The RT-PCR products were digested with *Bam*HI and the digestion products were analyzed by agarose gel electrophoresis. *Bam*HI has specificity for genome segment S6 of AHSV-4, with one site present in the genome segment, and does not cleave within the S6 genome segment of AHSV-1. Size markers (M) in base pairs are indicated.

Fig. 5. Plasmid-based AHSV-4 reverse genetics system driven by a plasmid-encoded T7 RNA polymerase. (A) Schematic of the experimental strategy. A monolayer of BSR or L929 cells is co-transfected with a modified 5-plasmid set, in which the T7 RNA polymerase expression cassette is incorporated into the genetic backbone of the pJAD-S2-S6 reverse genetics plasmid to yield pJAD-S2-S6-T7pol. In cells co-transfected with the 5 plasmids, T7 RNA polymerase is expressed under control of a CMV promoter, which induces expression of transcripts corresponding to the native AHSV-4 positive-sense transcripts from the plasmids. After incubation for 3 days, recombinant viruses are recovered by plaque assays of the transfection cell lysates on BSR cells. (B) Plaque formation by recovered AHSV-4 viruses generated with the modified 5-plasmid reverse genetics system using BSR and L929 cells, as indicated in the figure. Mock-transfected cells were included as controls. (C) Comparison of virus recovery with the modified 5-plasmid system using BSR and L929 cells. Virus titres in supernatants of co-transfected BSR or L929 cells were determined at different time post-transfection by plaque assays on BSR cells. The results are presented as the mean titres of three independent experiments and error bars indicate the standard deviation. (D) Electropherotypes of the recovered viruses obtained by electrophoresis of viral dsRNA from wild-type (WT) AHSV-4 and dsRNAs obtained from recombinant AHSV-4 viruses recovered with the modified 5-plasmid system in BSR cells (lane 1) and L929 cells (lane 2). The non-denaturing polyacrylamide gel was stained with ethidium bromide to visualize the viral genome segments (S1-S10).

Fig. 6. Comparison of virus recovery using the 10-plasmid, 5-plasmid and modified 5-plasmid AHSV-4 reverse genetics systems. BSR-T7 cells were co-transfected with the 10-plasmid set or 5-plasmid set, and BSR cells were co-transfected with the modified 5-plasmid set. The titres of virus released into the supernatant at different times post-transfection were determined by plaque assays on BSR cells. The results are presented as the mean titres of three independent experiments and error bars indicate the standard deviation.

Figure 1

A

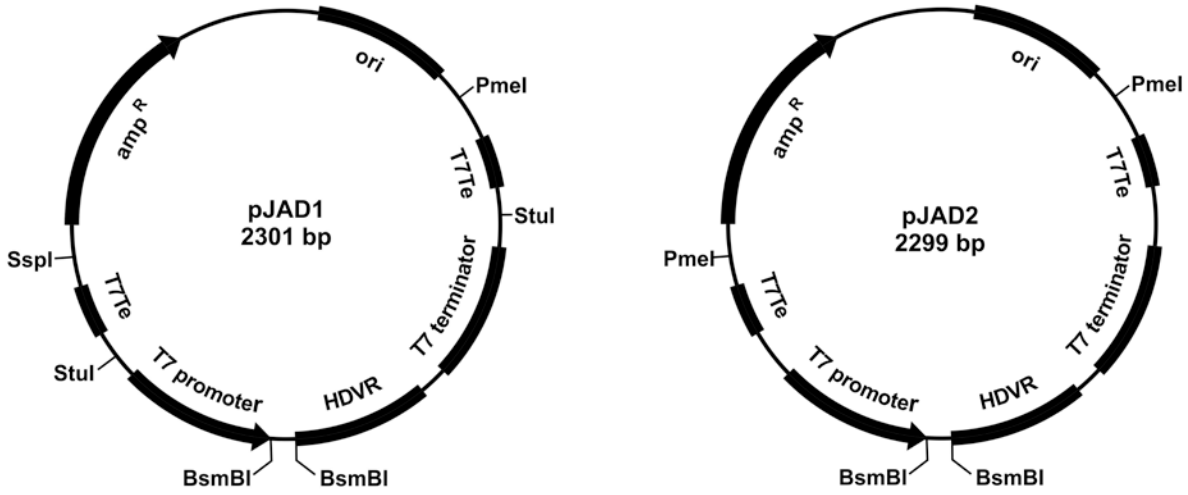
pJAD1
2301 bp
ori
PmeI
T7Te
StuI
T7 terminator
HDVR
BsmBI
BsmBI
T7 promoter
StuI
T7Te
SspI
amp R
pJAD2
2299 bp
ori
PmeI
T7Te
T7 terminator
HDVR
BsmBI
BsmBI
T7 promoter
PmeI
T7Te
amp R

B

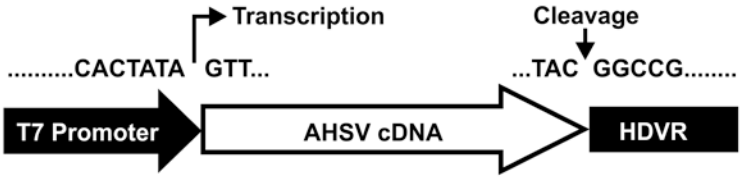
Transcription
Cleavage
.....CACTATA GTT...
...TAC GGCCG.....
T7 Promoter
AHSV cDNA
HDVR

Figure 2

A

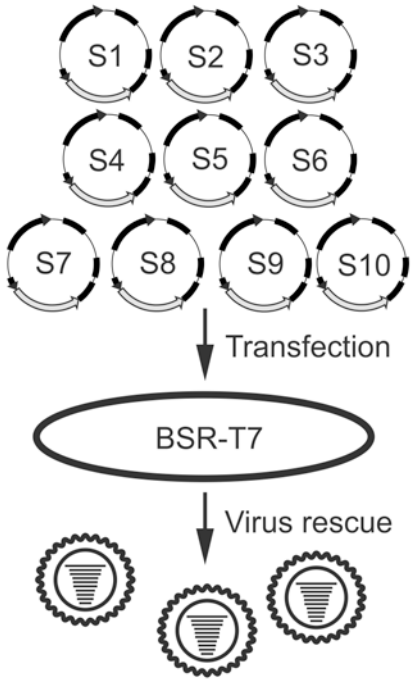

B

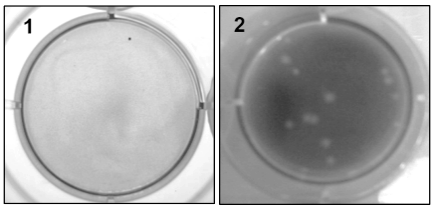

C

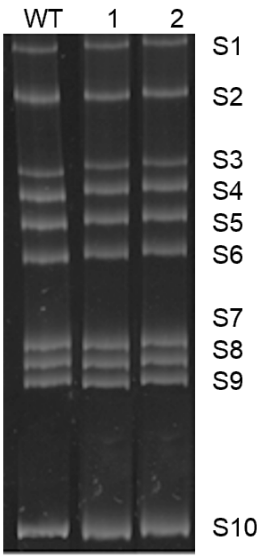

D

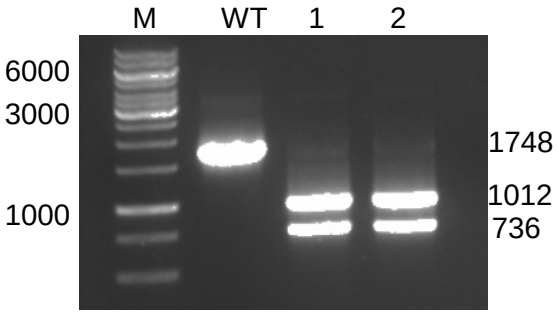

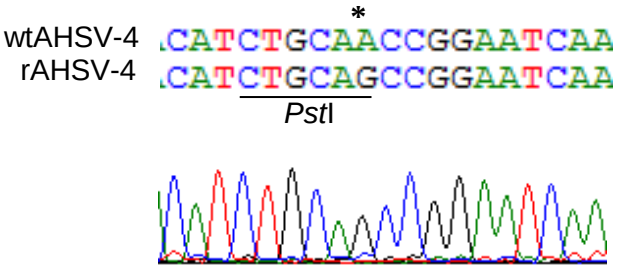

E

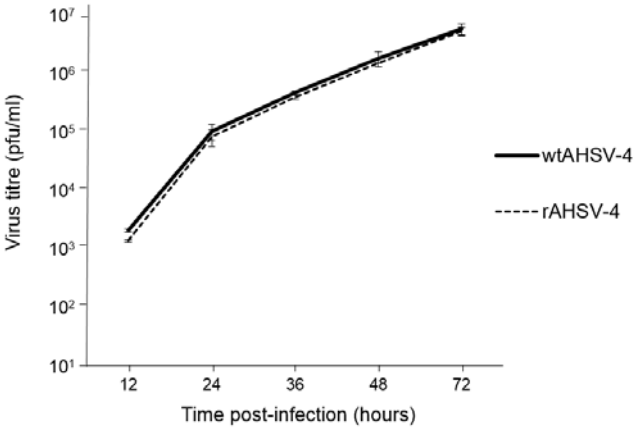
Virus titre (pfu/ml)
10⁷
10⁶
10⁵
10⁴
10³
10²
10¹
12
24
36
48
72
Time post-infection (hours)
wtAHSV-4
rAHSV-4

Figure 3

A

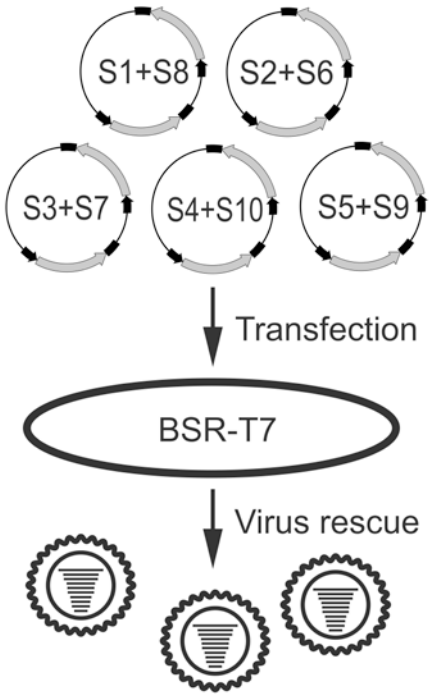

B

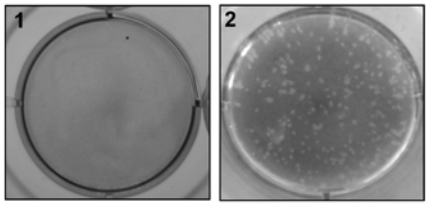

C

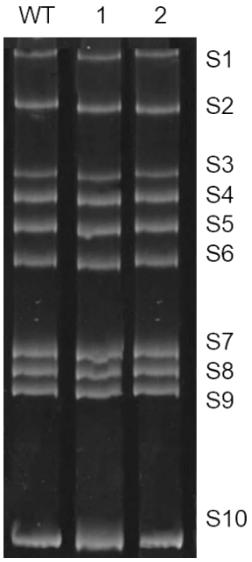

D

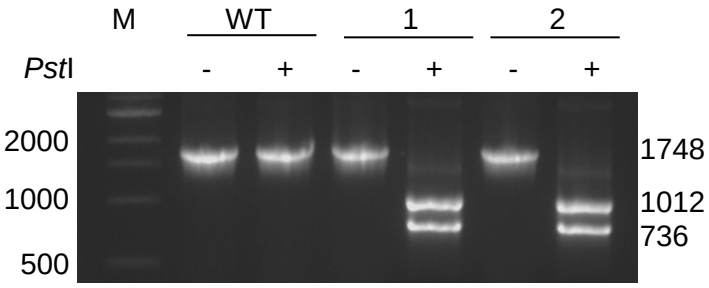

Figure 4

A

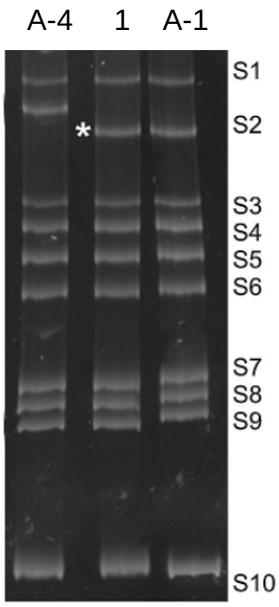
A-4
1
A-1
S1
S2
S3
S4
S5
S6
S7
S8
S9
S10
*

B

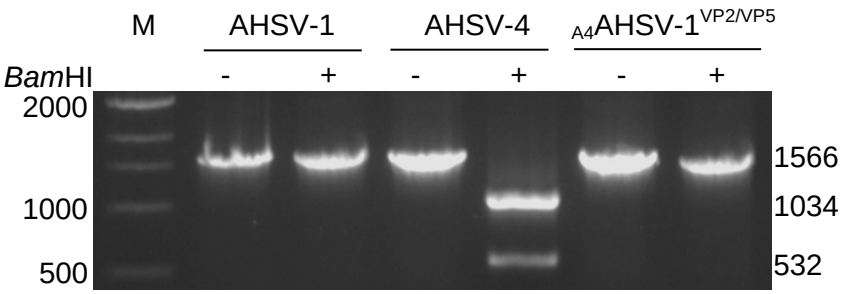
M
AHSV-1
AHSV-4
A4AHSV-1VP2/VP5
BamHI
-
+
-
+
-
+
2000
1000
500
1566
1034
532

Figure 5

A

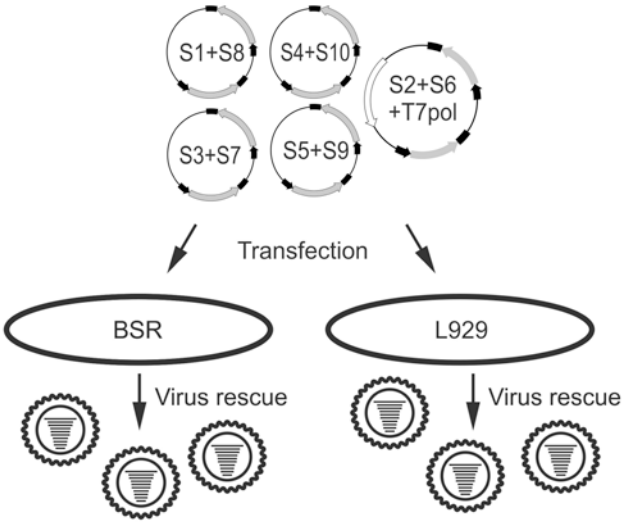

B

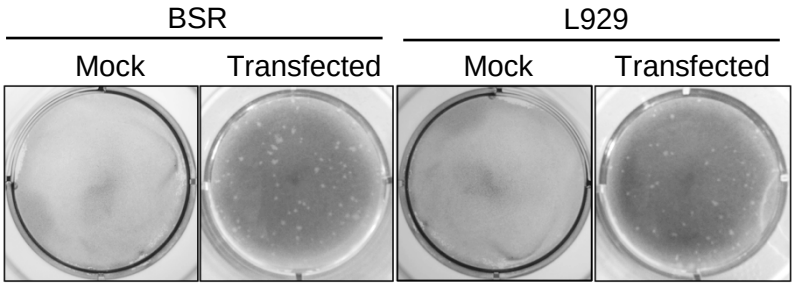

C

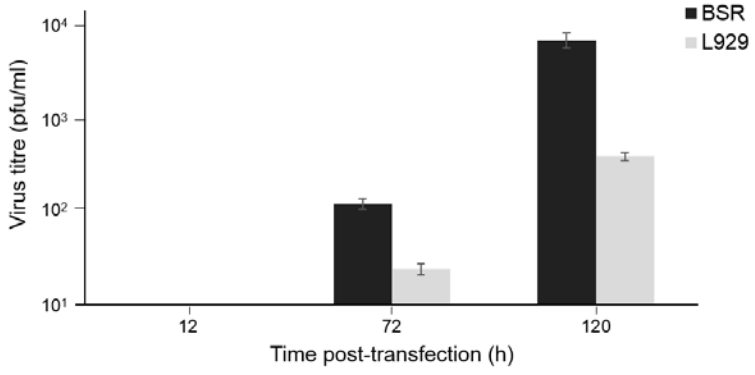

D

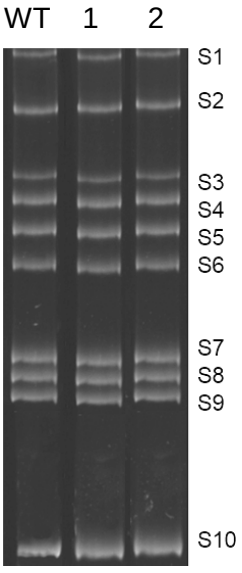

Figure 6

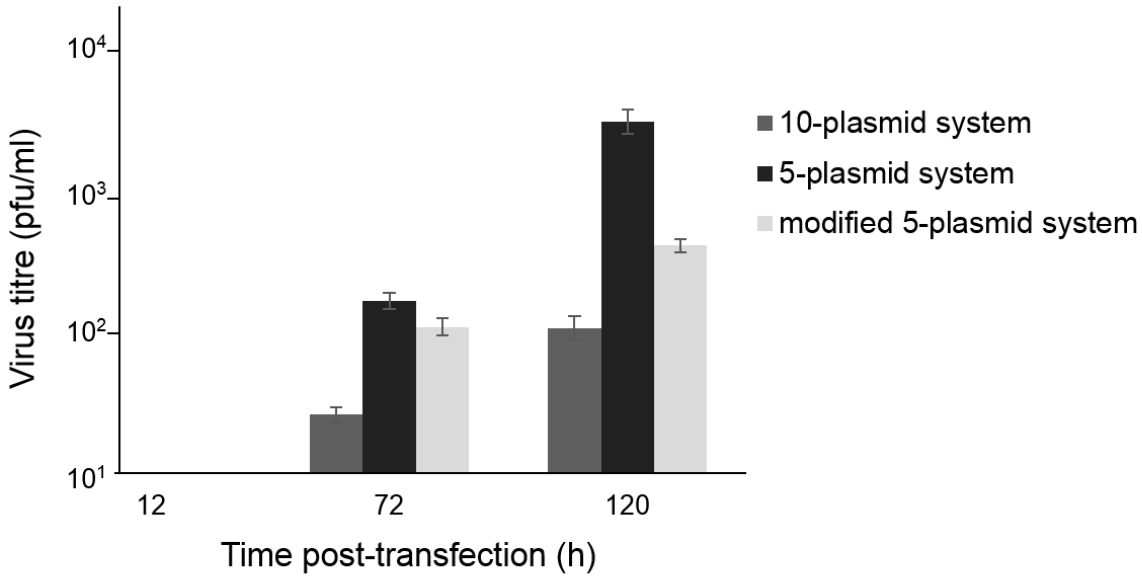
Virus titre (pfu/ml)
10^4
10^3
10^2
10^1
12
72
120
Time post-transfection (h)
10-plasmid system
5-plasmid system
modified 5-plasmid system